Arch. Metall. Mater. **62** (2017), 2, 807-814

DOI: 10.1515/amm-2017-0120

T. DYL*#

THE NUMERICAL AND EXPERIMENTAL ANALYSIS OF BALLIZING PROCESS OF STEEL TUBES

This paper presents chosen results of experimental and numerical research of ballizing process of the steel tubes. Ballizing process is a method of burnishing technology of an internal diameter by precisely forcing a ball through a slightly undersized pre-machined tubes. Ballizing process is a fast, low-cost process for sizing and finishing tubes. It consists of pressing a slightly oversized ball through an unfinished tube to quickly bring the hole to desired size. The ball is typically made from a very hard material such as tungsten carbide or bearing steel. Ballizing process is by cold surface plastic forming of the surface structure, thereby leaving a layer of harder material and reducing its roughness. After theoretical and experimental analysis it was determined that the smaller the diameter of the balls, the bigger intensity of stress and strain and strain rate. The paper presents influence of ballizing process on the strain and stress state and on the surface roughness reduction rate of the steel tubes.

Keywords: numerical analysis, strain and stress state, burnishing (surface plastic forming), ballizing process, steel tubes

1. Introduction

The burnishing process is a technology of surface plastic forming of machine parts used in the metallurgical industry, machinery and shipbuilding, etc. As the burnishing tools hard and smooth balls, rolls, and disks are used. Flat surfaces and cylindrical shapes can be burnished. Outer and inner surfaces in cylindrical shapes can be burnished. In advanced manufacturing, it is important to obtain good quality products. Therefore, it is used to carry out the finishing of machine elements.

The burnishing process is a finishing of tubes, which has a number of advantages. This treatment allows to increase the dimensional accuracy of holes and to decrease surface roughness parameters, increasing the hardness of the surface layer and forming compressive residual stresses. It is also important that the burnishing technology allows machining holes with a lack of straightness of the axis. The advantages of burnishing may also be considered in terms of high performance and relatively easy technological instrumentation. The tools used for burnishing include special broach plungers in variety of shapes and bearing balls. The beneficial effect of treating holes during burnishing process on the state of the surface layer and the accuracy of the machined holes are used for products made of unalloyed steel, steel alloys and stainless steel, copper alloys, and titanium alloys. Burnishing process is most often used for machining of circular cross section holes with a diameter from a few tenths of millimeter to about one hundred. In the papers [1-4] the usefulness of burnishing process (ballizing process) as a finishing hole machining sliding bearings was confirmed. It is important that special burnishing elements in the form of beads used as a tool for broaching were prepared.

Developed by using artificial neural networks [5], the model of stress distribution in the surface layer of workpieces can be used to expand the burnishing process control system, which may advantageously influence the quality of the machined elements used for the machine construction.

In available professional literature theoretical analysis of ballizing process by using the finite element method hasn't been found. The finite element method is used for simulation of different plastic workings: rolling, forging and pressing, drawing and other [6-12]. Numerical analysis based on the elastic and elastic/visco-plastic bodies is used for theoretical analysis of a contact surface of the spherical tool and the workpiece [13-15]. In the paper numerical analysis of ballizing based on elastic – plastic bodies was made. The state of stress and strain in the surface layer after ballizing can be determined using the finite element method.

2. Methodology of science research

The aims of ballizing process can be as follows: surface finish processing – predetermined reduction of surface irregularities after treatment prior to burnishing; strengthening processing – producing specific changes in the physical properties of the material in the surface layer of the object, causing it to be resistant to operation factors such as fatigue, wear, corrosion and others; dimension and surface finish treatment – a predetermined in-crease in dimensional accuracy, whilst reducing

* GDYNIA MARITIME UNIVERSITY, FACULTY OF MARINE ENGINEERING, DEPARTMENT OF MARINE MAINTENANCE, MORSKA STREET 81-87, 81-225 GDYNIA, POLAND

Corresponding author: dylu@am.gdynia.pl

surface roughness to the required value. Ballizing process tube hole using mandrel, lubricated with engine oil, was carried out on a hydraulic press PH-16 in the Laboratory of Plastic Working in Department of Marine Maintenance, Faculty of Marine Engineering, Gdynia Maritime University. Experimental and numerical research was conducted for steel samples (1.0503). The samples had the form steel sleeves, among which you can distinguish between four sets of samples. Internal diameters of samples from each set were made by boring in three dimensions. The largest internal diameter of a set of samples was about 0.1 mm smaller than the diameter of the tool. Two more samples from a given set of internal diameters were smaller than the ball diameter by 0.2 mm and 0.3 mm. In the figure 1 is shown schema burnishing process by ball. Ballizing process is pushing ball bearing steel (1.3567) through the tubes (Fig. 1).

Theoretical analysis of the ballizing carried out in numerically. For the calculations used program Forge® [16] based on the finite element method. Computer simulations were carried out at the Institute of Metal Forming and Safety Engineering, Faculty of Production Engineering and Materials Technology, Technical University of Czestochowa. The computer simulations were carried out with steel samples C45 (1.0503). The external diameter $D = 30 \div 45$ mm and internal $d_0 = 15.56 \div 33.22$ mm and diameter of balls bearing $d = 15.86 \div 33.32$ mm was used. The coefficient of sliding friction of steel on steel is 0.1, it has been selected on the basis of the literature [17,18]. The use of a commercial software Forge®, which is based on the finite element method and has built-in thermo-mechanical models, requires defining the boundary conditions. For the boundary conditions are: properties of a material, the conditions of friction, kinetic parameters and thermal properties and tools. Model of ballizing process of the steel tubes is shown in Figure 2.

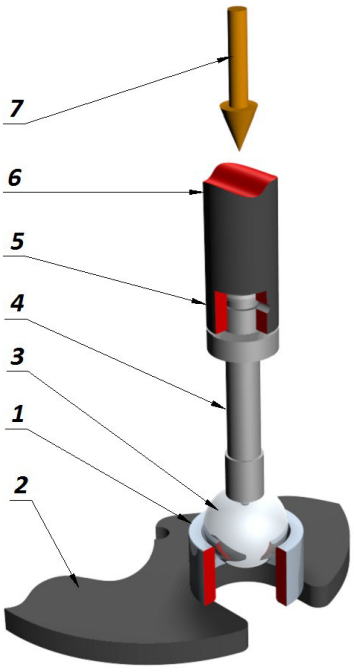

Fig. 1. Schema of ballizing process, 1 – tube, 2 – basis of hydraulic press PH-16, 3 – ball, 4-guide-pin ball, 5 – mounting socket, 6 – punch of hydraulic press PH-16, 7 – direction of pushing force

The commercial software Forge® were used a model consisting of a finite element mesh, whose base element is a triangle. The friction forces been model on the basis of the solution Tresca [17,18]. For the computer simulation, the input data are as follows: the initial temperature is the ambient temperature, the heat exchange coefficient between the workpiece and the tool 200 W/Km^2, the heat exchange coefficient between the material and the air 10 W/Km^2. Due to limitations of the software used movable third element in the form of a thin disc sliding burnishing tubes. The use of a moveable tubes on the beads did not affect the accuracy of the calculations and only affect the calculation time by increasing the number of elements in the node which calculations are performed. Computer simulations were carried out in a three-dimensional reference system.

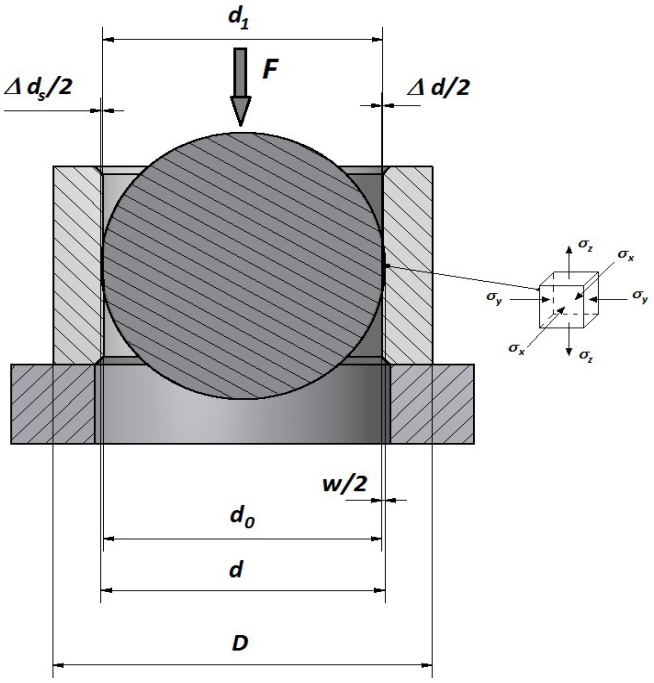

Fig. 2. Model of ballizing process, D – external diameter tube, d – outer diameter of the ball, d_0 – diameter inner tube before burnishing, d_1 – diameter inner tube after burnishing, w – reduction ratio, Δd – absolute plastic strain, Δd_s – absolute elastic strain

The Norton-Hoff visco-plastic formulation is defined from the visco-plastic potential convenient to derive the variation and the weak forms equivalent to the equilibrium equations. The Norton-Hoff state of visco-plastic materials is expressed by the equation [18-22]:

$$S_{ij} = 2K_0\left(\varepsilon + \varepsilon_0\right)^{n_0} \cdot e^{(-\beta_0 \cdot T)}\left(\sqrt{3}\,\dot{\varepsilon}_i\right)^{m_0 - 1}\dot{\varepsilon}_{ij} \qquad (1)$$

where: S_{ij} – stress tensor deviator, $\dot{\varepsilon}_{ij}$ – strain rate tensor, $\dot{\varepsilon}_i$ – strain rate intensity, ε – strain intensity, ε_0 – based strain, T – temperature, K_0, m_0, n_0, β_0 – material constants specific to the material considered.

The yield stress dependence of strain intensity, strain rate and temperature used for the theoretical research is approximated by extended Hensel-Spittel [23] formula expressed as:

$$\sigma_p = K_0\, e^{m_1 T}\, \varepsilon^{m_2}\, \dot{\varepsilon}_i^{\,m_3}\, e^{\frac{m_4}{\varepsilon}} \tag{2}$$

where: σ_p – yield stress, ε – strain intensity, $\dot{\varepsilon}_i$ – strain rate intensity, T – temperature, K_0, m_1, m_2, m_3, m_4 – coefficients of the function.

In order to determine the coefficients of the equation (2) performed approximation results of the plastometric test results made on the DIL 805 A/D system in the Institute of Metal Forming and Safety Engineering, Faculty of Production Engineering and Materials Technology, Technical University of Czestochowa. Coefficients used in equation (2) for both materials are given in Table 1.

TABLE 1

Parameters of function (2) for: ball bearing steel (1.3567) and steel samples (1.0503)

Steel	K_0	m_1	m_2	m_3	m_4
C45 (1.0503)	1521.306	–0.00269	–0.12651	0.14542	–0.05957
20CrMo4 (1.3567)	1232.9863	–0.00254	–0.05621	0.1455	–0.0324

Table 2 shows examples of the geometrical parameters for the steel tubes after ballizing process. The relative plastic deformation for ballizing is expressed by the formula [18]:

$$\varepsilon_{np} = \frac{d - d_0}{d_0} \cdot 100\% \tag{3}$$

where: d – outer diameter of the ball, d_0 – diameter inner tube before burnishing.

TABLE 2

Geometrical parameters and strain ratio of the steel tube holes after ballizing process

No of samples	D, [mm]	d [mm]	d_0, [mm]	d_1, [mm]	Δd, [mm]	w, [mm]	ε_{np}, [%]
101	45	33.32	33.22	33.28	0.06	0.1	0.3
102	45	33.32	33.12	33.29	0.17	0.2	0.6
103	45	33.32	33.02	33.29	0.27	0.3	0.9
201	35	22.00	21.90	21.97	0.07	0.1	0.5
202	35	22.00	21.80	21.97	0.17	0.2	0.9
203	35	22.00	21.70	21.97	0.27	0.3	1.4
301	30	15.86	15.76	15.84	0.08	0.1	0.6
302	30	15.86	15.66	15.82	0.16	0.2	1.2
303	30	15.86	15.56	15.83	0.27	0.3	2.0

The measurements were performed according to the principles contained in ISO standards. A number of parameters of surface roughness after burnishing were determined; among other things, parameters were defined associated with the material share curve.

Parameter (*Rpk*) variable of the reduced peak height (which should be the lowest) is characteristic for the upper surface layer that quickly undergoes abrasion after the commencement of, for example, engine running. Reduced depth of roughness profile valley is described by (*Rvk*) parameter (which should be the highest). It is a measure of the working surfaces ability to keep the lubricant in the valleys created mechanically. Parameter (*Rk*) defines the core roughness depth (which should be the lowest).

Surface roughness after ballizing was measured with a profilometer Hommel – Tester T1000 in the Faculty of Marine Engineering Gdynia Maritime University. The assumed measurement section length of test sample was 4.8 mm and 0.8 mm for the elementary section.

3. Results of numerical simulation

The strain hardening of the material structure of the surface layer is obtained by cold plastic deformation, this improves the fatigue strength. After the burnishing are constituted compressive residual stresses in the surface layer that result from increased specific volume of the material in a plastic state. The maximum absolute value stresses occur near the surface of the burnishing [18]. Resistance to fatigue is one of the exploitation properties of machines, changing preferably by burnishing. Can be determined based on the relationship between the parameters and the strain state in the surface layer material. It is therefore important to determine the strain state in the tubular elements widely used in the machinery and shipbuilding and metallurgical industry. Figure 3 shown the distributions effective strain for computer simulation using a Forge® for the burnishing ball diameter $d = 22.00$ mm for reduction ratio $w = 0.3$ mm for relative plastic deformation $\varepsilon_{np} = 1.4\%$ (sample number 203).

Because of nature of the burnishing shown axisymmetric distributions of selected strains in the middle of the tube hollow on the longitudinal section was presented.

Figures 4-6 shows the distributions effective strain intensity and strain rate intensity of the burnishing ball diameter $d = 15.86 \div 33.32$ mm and reduction ratio 0.3 mm.

Based on the results shown in Figures 4-6, it can be concluded that the effective strain and strain rate depend on the outer diameter of the ball. For smaller diameters balls of strain take the greatest value. It can be concluded that the intensity of the deformation in the outer layer of the tube hollow from the inside of contact with the ball increases with the reduction ratio. Conversely the intensity is proportional dependence of the deformation and the diameter of the balls. Depending similarly occur in the event of deformation. For larger values of the diameter of the balls as well as the intensity of deformation strain rate values take smaller and smaller diameter of the balls reach the higher values. This character of strain distribution is determined by the average stresses intensity values increase with decreasing diameter of the balls (Fig. 7). This is directly related to the decrease in the surface area of contact deformation element burnishing the inner wall of the steel tube hollow.

Depending residual stress as a function of: the outer diameter of the ball, absolute and relative plastic deformation for the burnishing set within 50 μm from the machined surface of the tube hollow and is shown in Figure 8.

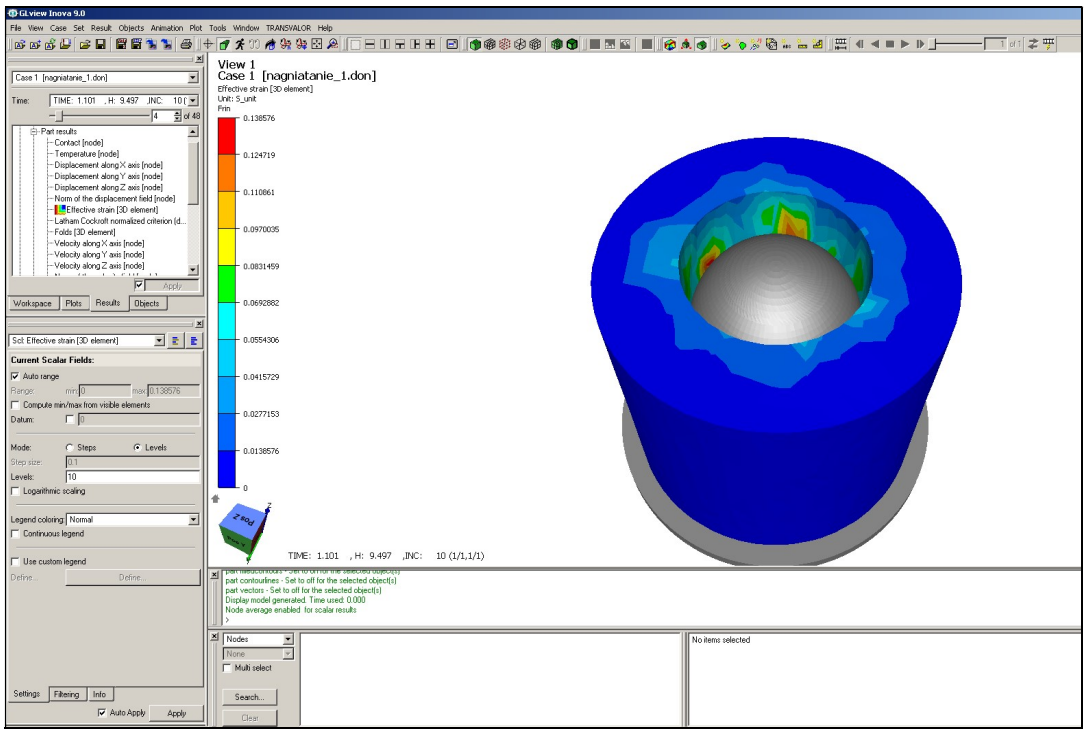

Fig. 3. The distributions effective strain intensity for computer simulation ballizing process using a Forge® for the sample number 203

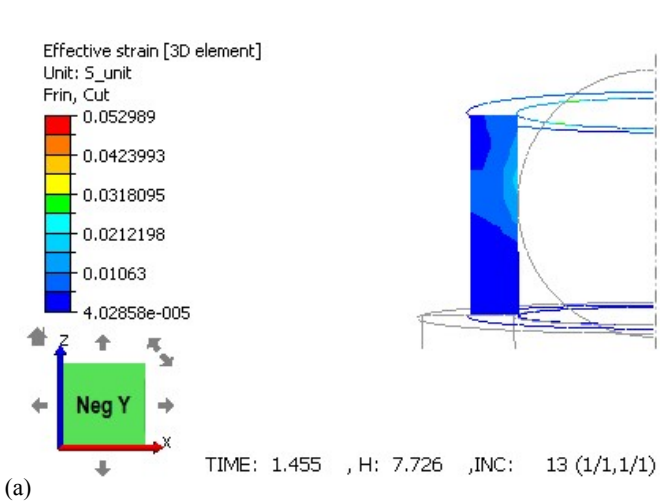

(a)

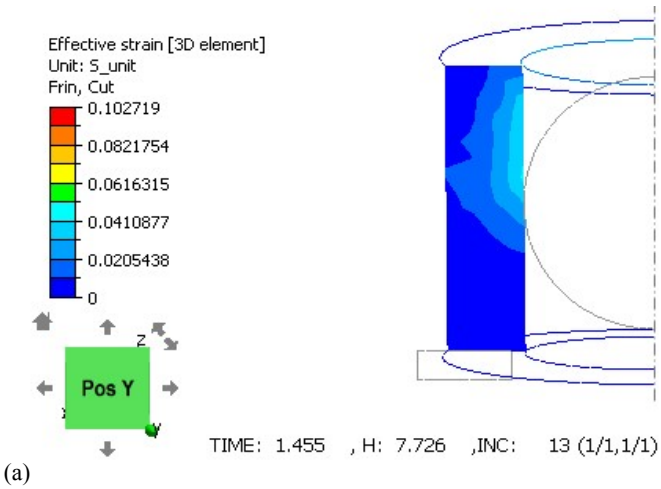

(a)

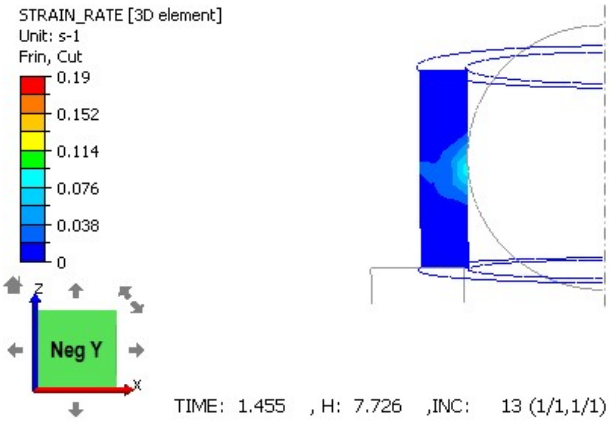

(b)

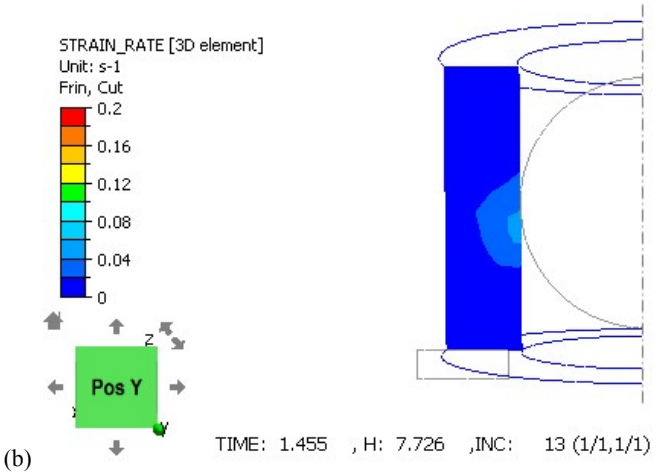

(b)

Fig. 4. The distribution of the effective strain intensity (a) and strain rate intensity (b) for ball diameter d = 33.32 mm and the reduction ratio w = 0.3 mm

Fig. 5. The distribution of the effective strain intensity (a) and strain rate intensity (b) for ball diameter d = 22.00 mm and the reduction ratio w = 0.3 mm

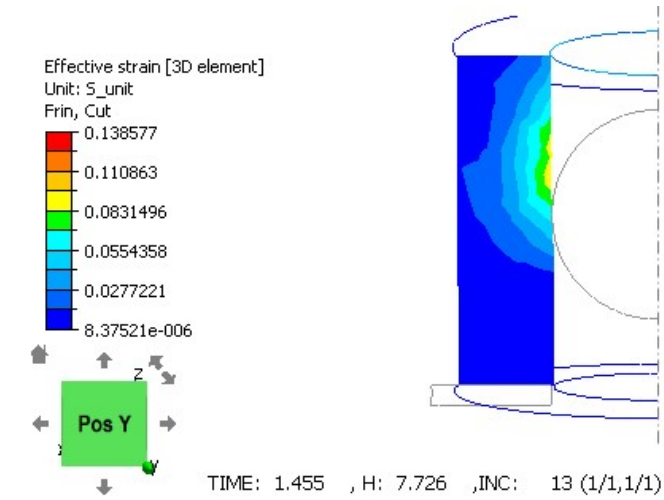

(a)

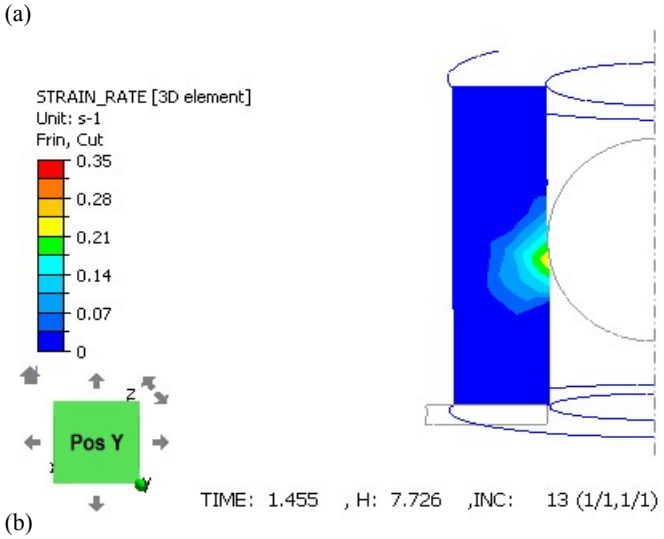

(b)

Fig. 6. The distribution of the effective strain intensity (a) and strain rate intensity (b) for ball diameter d = 15.86 mm and the reduction ratio w = 0.3 mm

With the increase in the value of the diameter of the ball burnishing strain value de-crease. Such nature of the deformation state is directly dependent on the state of stress occurring in the outer layer of the tube hollow subjected to burnishing.

Based on the analysis results shown in Figure 8 it can be concluded that the residual stresses are numerically calculated dependent on two variables: the outer diameter of the balls and the predetermined strain for burnishing. It can be concluded that the higher relative plastic deformation and with the increase of the reduction ratio, while reducing the diameter of the ball there is an increase the absolute value of the compressive residual stress in the inner surface layer of the tube hollow.

In order to determine the depth of the zone of plastic deformation used in numerical analysis based on the finite element method. The paper was determined as a numerical solution for contact and deformation of bodies on the basis of the theory of plasticity and elasticity. Based on numerical analysis of the equations can be calculated the depth of plastic deformation zone. For the required boundary conditions and specific areas of research, determined on the basis of their own numerical sliding burnishing the relationship between the depth of the zone of plastic deformation and the deformation and reduction ratio shown by the equation:

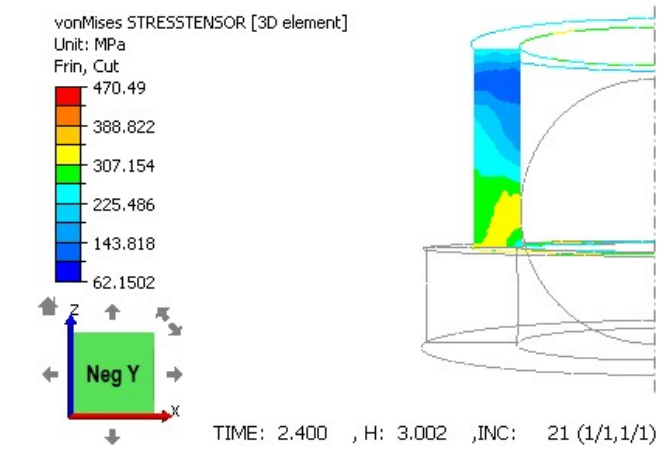

(a)

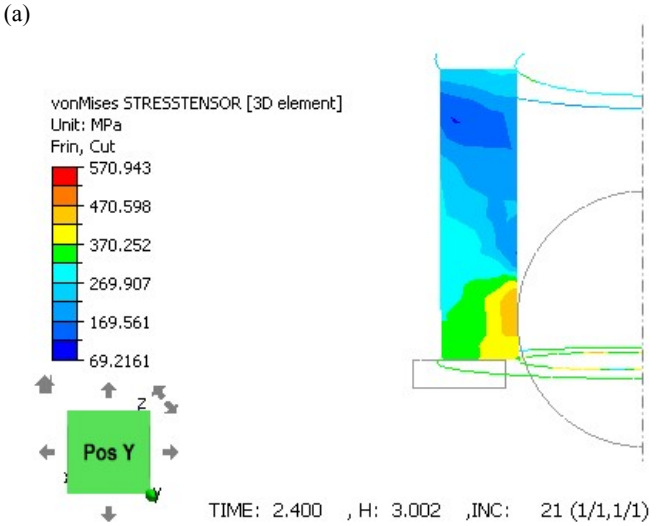

(b)

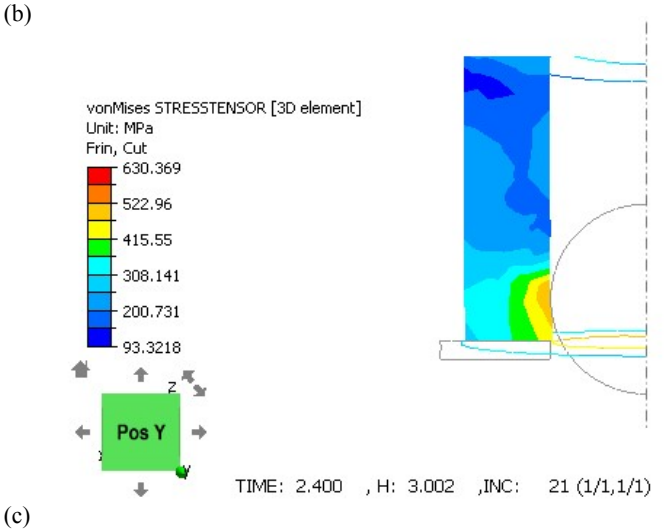

(c)

Fig. 7. The distribution of the stresses intensity for ball diameter: d = 33.32 mm (a) and d = 22.00 mm (b) and d = 15.86 mm (c) for the reduction ratio w = 0.3 mm after ballizing process

$$h_\delta = 0.756\, w^{1.667} \tag{4}$$

where: h_δ – depth of deformation zone, w – reduction ratio.

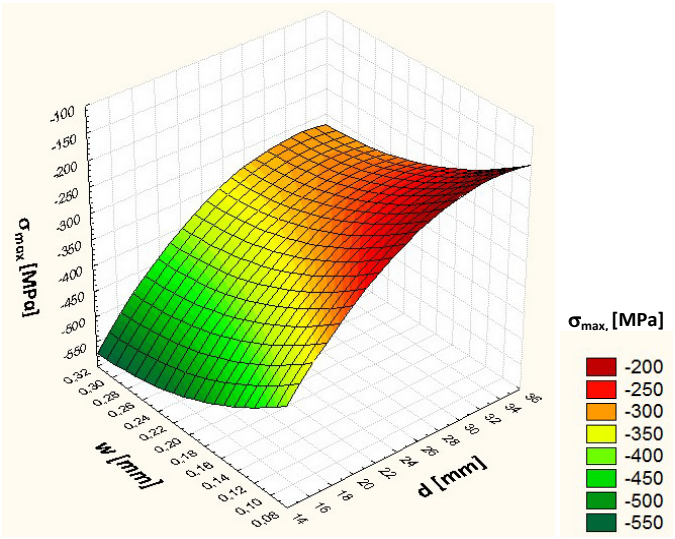

Fig. 8. The residual stresses – σ_{max}, as a function of: d – diameter of the ball and w – reduction ratio for ballizing process

4. Experimental study

The measurements of roughness were performed and then on the basis of parameters of surface roughness after burnishing the surface roughness reduction rate were determined [18]:

$$K_{Ra} = \frac{R'a}{Ra} \tag{5}$$

where: $R'a$ – arithmetic mean deviation of the surface roughness profile before ballizing, ($R'a$ = 4.17 μm), Ra – arithmetic mean deviation of the surface roughness profile after ballizing.

On the basis of measurements of the roughness profile determined to improve smoothness. After conducting research burnishing process tube holes of C45 steel (1.0503) it was determined that effectively replaces the machining such as grinding, reaming, honing and lapping – but without the abrasive contaminants in the surface layer characteristic of the grinding. Figure 9 shows the Abbott-Firestone curve and the arithmetical mean deviation of the assessed profile after ballizing process for relative plastic deformation ε_{np} = 1.4%. For sample number 203 (ε_{np} = 1.4%) after burnishing determined that the arithmetical mean deviation of the assessed profile and the Abbott-Firestone curve surface roughness parameters take the smallest value (Table 3). After burnishing process the results of measurements of roughness parameters, we can conclude that the improved bearing capacity inner surface tube holes. Based on the results of measurements parameters of surface roughness after burnishing process it can be concluded that with increasing relative plastic deformation decreasing surface roughness.

The depth of the roughness profile core (Rk) and the reduced elevation height (Rpk) take the lowest values possible, while the reduced depth of recesses of the roughness profile (Rvk) takes the greatest value possible for samples number 203 and 303 when tube holes was burnished for relative plastic deformation ε_{np} = 1.4%÷2.0%.

We can conclude that the greater the degree of deformation of the inner surface tube holes the more decrease the values of roughness profile.

After ballizing process experimental studies determined the dependence between relative plastic deformation (ε_{np}) and surface roughness reduction rate (K_{Ra}).

The data presented in Figures 10 shows that with an increase in the relative plastic deformation , the value of the surface roughness reduction rate increases. The increase in value surface roughness reduction rate is dependent on the applied degree of relative plastic deformation. For a given range ε_{np} = 0.3÷2.0%. can to determine the change of roughness with the known values of arithmetic mean deviation of the surface roughness profile before and after burnishing process.

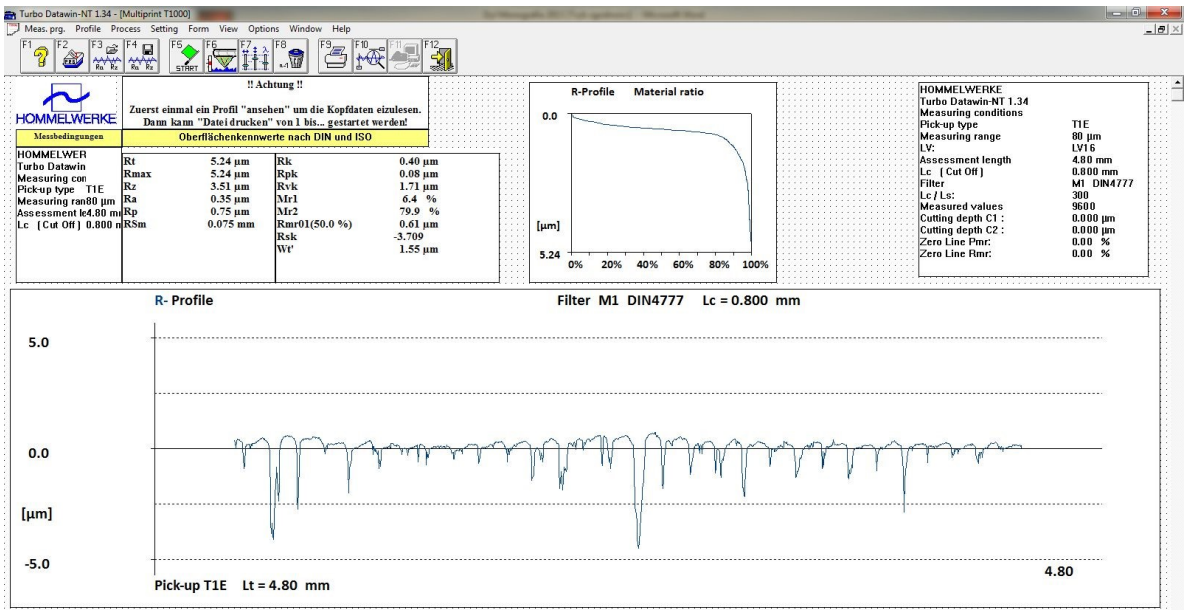

Fig. 9. The Abbott-Firestone (Material Ratio) curve and the profile roughness after ballizing process for relative plastic deformation ε_{np} = 1.4% (sample No 203)

TABLE 3

The parameters of surface roughness for the steel tube holes after ballizing process

No of samples	*Rt* [mm]	*Rz* [mm]	*Ra* [mm]	*Rp* [mm]	*RSm* [mm]	*Rk* [mm]	*Rpk* [mm]	*Rvk* [mm]	*Mr*1 [%]	*Mr*2 [%]	*Rmr*01 [mm]
101	12.39	8.98	1.57	2.64	0.12	1.48	0.34	5.40	4.9	66.1	1.90
102	12.38	8.85	1.51	2.89	0.09	1.69	0.28	5.03	6.0	67.2	2.23
103	9.77	7.72	1.39	2.27	0.08	1.58	0.15	3.94	2.7	60.3	1.58
201	9.16	7.65	1.24	2.18	0.12	0.93	0.27	4.50	6.1	67.1	1.48
202	8.25	7.91	0.84	1.84	0.11	0.58	0.25	4.13	8.6	77.0	1.50
203	5.24	3.51	0.35	0.75	0.08	0.40	0.08	1.71	6.4	79.9	0.61
301	7.97	6.80	1.16	1.43	0.10	0.85	0.15	4.2	3.2	67.4	0.76
302	6.82	4.86	0.64	1.17	0.08	0.54	0.12	2.4	5.8	69.5	0.84
303	6.67	3.90	0.32	0.84	0.07	0.33	0.20	1.9	10.6	83.8	0.69

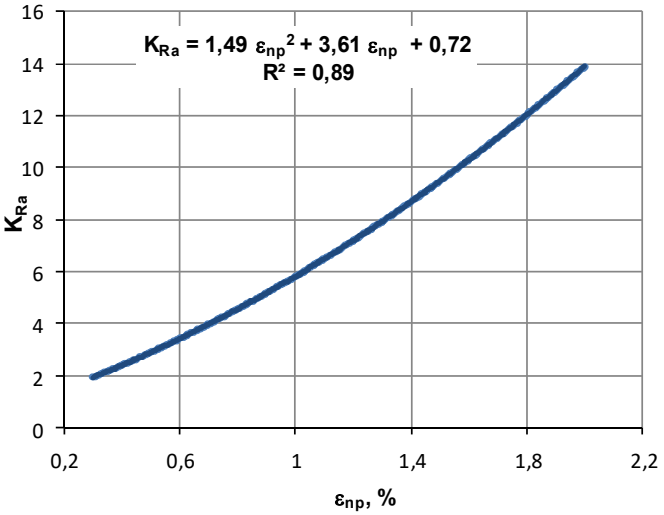

Fig. 10. The influence of the relative plastic deformation (ε_{np}) on surface roughness reduction rate (K_{Ra})

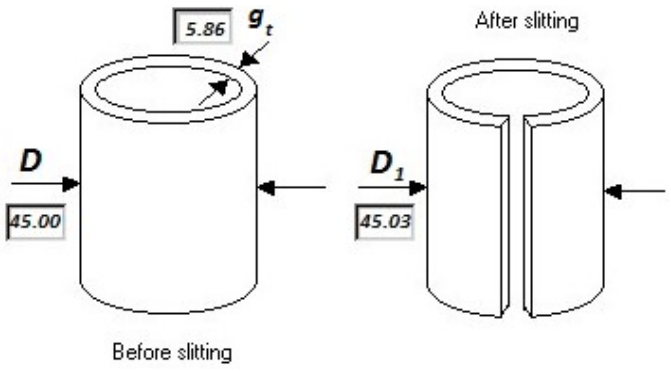

Fig. 11. Scheme of tube before and after slitting after ballizing process

5. Comparison of the numerical and experimental study

Comparison of results of experimental and theoretical research was made by the residual stresses analysis. After ballizing process were determined residual stresses. Sectioning to allow relaxation of residual stress in actual components where stresses are thought to be present can be performed by several methods, from simple saw cutting to the more sophisticated compliance method. One of the simplest methods of determination the circumferential hoop residual stress in tubes is to make slitting along the ring, which was cut off from the tube. Operation of slitting (Fig. 11) causes distortion of the ring as a result of release and redistribution of circumferential residual stress [18,24].

The residual stresses are described by the following formula [18,24]:

$$\sigma_C = E \cdot g_t \left(\frac{1}{D} - \frac{1}{D_1} \right) \tag{6}$$

where: E – Modulus Elasticity, (E = 210 GPa, for steel), g_t – thickness of the wall, mm, D – outer diameter tube before slitting after ballizing, D_1 – outer diameter tube after slitting.

In the works [24] were presented ranges of residual stresses acceptability for: $\sigma_C < 35$ MPa – acceptable; $\sigma_C = 35$-70 MPa – borderline; $\sigma_C > 70$ MPa – unacceptable.

After the tests were cut along a sample and an external diameter were measured and calculated residual stress.

The experimental study was calculated from the formula (6) residual stress, whose value was equal to, $\sigma_C = 18.22$ MPa (for sample 103), $\sigma_C = 22.32$ MPa (for sample 203), $\sigma_C = 33.15$ MPa (for sample 303), is the value to an acceptable $\sigma_C < 35$ MPa.

Then the results of calculations of residual stresses occurring in the tubes compared to the stress values obtained by numerical studies [18] and identified a high consistency of results. Residual stresses were calculated numerically after carried out computer simulations of the ballizing process were equal: $\sigma_C = 18.82$ MPa (for sample 103), $\sigma_C = 23.83$ MPa, (for sample 203), $\sigma_C = 36.68$ MPa, (for sample 303). These values of residual stresses in the tubes after burnishing was calculated by deflection method remaining that was smaller of the permissible stresses $\sigma_C < 35$ MPa.

Numerical modeling has been verified experimentally determined and high consistency of results calculated numerically and designated deflection method of residual stresses as a function of tool geometry and the relative plastic deformation and reduction ratio.

Conclusions

The numerical analysis is determining that the reduction ratio has significantly influenced on the state strain of the inner tube holes after ballizing process. An increase in the value of reduction ratio, the value of the effective strain increases. After burnishing simulations can be concluded that the most intense nature of the surface of an elastically deformable material contact with the ball is the state of effective strain and strain rate. The values of the deformation and intensity stresses is propagated in the material and tool contact. Examined the cross-section of the tube hollow can be seen that the area is characteristic of the occurrence of deformation and stress tensors maximum value at a certain depth from the surface of the workpiece, but not more like half of the wall thickness of the tubes.

After the studies carried out, it was determined that the relative plastic deformation has significantly influenced on the alteration roughness of the inner tube holes after ballizing process. An increase in the value of relative plastic deformation, the value of the surface roughness reduction rate increases. After conducting research burnishing tube holes of C45 steel it was determined that effectively replaces the machining such as grinding, reaming, honing and lapping – but without the abrasive contaminants in the surface layer characteristic of the grinding. On this basis, knowing the initial roughness and the degree of deformation burnishing process you can specify the expected roughness recommended by the producer of a steel tube holes.

After analyzing the numerical and experimental of ballizing process can be conclude that can effectively specify state of strain required for planning finishing abrasive tube for the piece production and small lot production.

REFERENCES

[1] M. Fattouh, Some Investigation on the Ballizing Process, Wear **134**, 209-219 (1989).

[2] S.Z. El-Abden, M. Abdel-Rahman, F.A. Mohamed, Finishing of non-ferrous internal surfaces using ballizing technique, Journal of Materials Processing Technology **124**, 144-152 (2002).

[3] P.K. Upadhyay, A.R. Ansari, P. Agarwal, Study and Analysis of Geometric Effect of Ball Burnishing Process of Different Materials and Evaluation of Forces and Strain for Ballizing Process, Current World Environment **7**, 101-108 (2012).

[4] T. Dyl, Ballizing process impact on the geometric structure of the steel tubes, Solid State Phenomena **199**, 384-389 (2013).

[5] J. Lipski, K. Zaleski, Modelling of residual stresses distribution in workpiece past ballizing process, Maintenance and Reliability **4**, 18-21 (2004).

[6] Z. Pater, J. Kazanecki, J. Bartnicki, Three dimensional thermo--mechanical simulation of the tube forming process in Diescher's mill, Journal of Materials Processing Technology **177**, 167-170 (2006).

[7] D.C. Chen, W.J. Chen, J.Y. Lin, M.W. Jheng, J.M. Chen, Finite element analysis of superplastic blow-forming of Ti-6Al-4V sheet into closed ellipcylindrical die, International Journal of Simulation Modelling **9**, 17-27 (2010).

[8] A. Gontarz, Z. Pater, A. Tofil, Numerical Analysis of unconventional forging process of hollowed shaft from Ti-6Al-4V, Journal of Shanghai Jiaotong University **16** (2), 157-161 (2011).

[9] J. Tomczak, Z. Pater, Analysis of metal forming process of a hollowed gear shaft, Metalurgija **51** (4), 497-500 (2012).

[10] H. Dyja, K. Sobczak, A. Kawałek, M. Knapiński, The analysis of the influence of varying types of shape grooves on the behaviour of internal material discontinuities during rolling, Metalurgija **52**, 35-38 (2013).

[11] M. Sayahi, S. Sghaier, H. Belhadjsalah, Finite element analysis of ball burnishing process: comparisons between numerical results and experiments, Int. J. Adv. Manuf. Technol. **67**, 1665-1673 (2013).

[12] Z. Pater, J. Tomczak, J. Bartnicki, M.R. Lovell, P.L. Menezes, Experimental and numerical analysis of helical-wedle rolling process for producing steel balls, International Journal of Machine Tools & Manufacture **67**, 1-7 (2013).

[13] L. Kukiełka, K. Kukiełka, A. Kułakowska, R. Patyk, L. Mąląg, L. Bohdal, Incremental modelling and numerical solution of the contact problem between movable elastic and elastic/visco-plastic bodies and application in the technological processes, Applied Mechanics and Materials **474**, 159-164 (2014).

[14] A. Rodriguez, L.N. Lopez de Lacalle, A. Celaya, A. Lamikiz, J. Albizuri, Surface improvement of shafts by the deep ball-burnishing technique, Surface & Coatings Technology **206**, 2817-2824 (2012).

[15] A.L. Vorontsov, The stress-strain state of hollow cylindrical workpieces when burnishing holes. Russian Engineering Research **2**, 108-114 (2007).

[16] FORGE® Reference Guide Release, Transvalor S.A. Parc de Haute Technologie Sophia-Antipolis 2002.

[17] T. Dyl, G. Stradomski, D. Rydz, Effect of the reduction ratio on the state strain of the steel tubes after burnishing broaching process, METAL 2014. 23rd International Conference on Metallurgy and Materials, Brno Czech Republic EU, 335-340 May 21-23 2014.

[18] T. Dyl, Numerical and experimental analysis of burnishing process using the theory of elasticity and plasticity, Monographs-Gdynia Maritime University, 130 Gdynia 2014.

[19] F.H. Norton, The creep of steel at high temperatures, McGraw-Hill London 1929.

[20] N.J. Hoff, Approximate analysis of structures in the presence of moderately large creep deformations, Quart. of Appl. Match. **12** (1), 49 (1954).

[21] D. Lochegnies, J.C. Gelin, A mixed variational formulation fort the solution of Norton-Hoff viscoplastic flows, Computers and Structures **65**, 177-189 (1997).

[22] V.L. Kolmogorov, V.P. Fedotov, A.V. Gorshkov, Three-dimensional analysis of the stress-strain state in the process of plastic deformation of metals, Journal of Materials Processing Technology **95**, 55-64 (1999).

[23] A. Hensel, T. Spittel, Kraft und Arbeitsbedarf Bildsomer Formgeburgs Verfahren, Lipsk 1979.

[24] H.W. Walton, Deflection methods to estimate residual stress, Handbook of Residual Stress and Deformation of Steel edited by G. Totten, M. Howes, T. Inoue, 89-98 (2002).